

# Determination of Ethanol Fuel Adulteration by Methanol Using Partial Least-Squares Models Based on Fourier Transform Techniques

Helena S. P. Carneiro,<sup>\*,†,‡</sup> Alex R. B. Medeiros,<sup>†</sup> Flavia C. C. Oliveira,<sup>‡</sup>  
Gustavo H. M. Aguiar,<sup>‡</sup> Joel C. Rubim,<sup>‡</sup> and Paulo A. Z. Suarez<sup>‡</sup>

Agência Nacional do Petróleo (ANP), SGAN 603 Módulo H, CEP 70830-902, DF, Brazil, and Laboratório de Materiais e Combustíveis (LMC)—Instituto de Química da Universidade de Brasília, Universidade de Brasília, CP 04478, 70904-970, DF, Brazil

Received January 9, 2008. Revised Manuscript Received March 19, 2008

The use of ethanol fuel is becoming worldwide and Brazil is the largest consumer of ethanol fuel as hydrated ethyl alcohol fuel (AEHC). Due to the similarities of the physical–chemical properties of ethanol and methanol, ethanol fuel is being adulterated with methanol. In the present work, we propose the use of partial least-squares regression (PLS) calibration models based on Fourier transform mid-infrared (FTMIR) and Fourier transform near-infrared (FTNIR) measurements as a fast, precise, and accurate method to evaluate the quality of AEHC as well as to detect its adulteration with methanol. Eighty mixtures of methanol/ethanol/water standards were prepared. Sixty were used for calibration, and twenty, for validation. The validation samples were also analyzed by gas chromatography flame ionization detection (GC-FID) to determine the ethanol and methanol content. The results have shown that among the two investigated spectroscopic techniques, PLS/FTNIR presented the best performance for the detection of methanol with a root-mean-square error of prediction (RMSEP % w/w) of 0.15 as compared to the value of 0.54 obtained by the FTMIR model, while the GC-FID results presented a prediction error of 0.52 (% w/w). The minimum detected net concentration of MeOH with the FTNIR model was ca. 0.51 (% w/w).

## Introduction

Ethanol's growing importance is related to the necessity to reduce greenhouse effects and the dependence on fossil fuels.<sup>1</sup> As such, many countries are now using ethanol as an alternative fuel since it can be obtained from renewable resources. Ethanol fuel has been used in Brazil since 1975 and is known as AEHC (hydrated ethyl alcohol fuel), and E85 (a blend of 85% ethanol and 15% gasoline) is currently used in Sweden and in ethanol flexible-fuel vehicles (FFVs) in the USA.

In 2006, the Agência Nacional do Petróleo, Gás Natural e Biocombustíveis (ANP), the Brazilian Federal Regulatory Agency for fuels, found that some AEHC commercialized in Brazil was adulterated with methanol.

Ethanol (EtOH) and methanol (MeOH) are alcohols with physical–chemical properties<sup>2</sup> that are very similar. Both are water soluble and colorless, and their densities are quite similar, 0.7937 (EtOH) and 0.7965 g/L (MeOH). These similarities and the lower prices of methanol in relation to ethanol are the main causes of AEHC adulteration with methanol, at least in Brazil. Methanol, however, is not allowed to be used as fuel in Brazil. Besides the fact that adulteration of AEHC with MeOH is a fiscal fraud in Brazil, it presents high toxicity and can cause temporary or permanent corneal<sup>3</sup> and pancreatic<sup>4</sup> damage or

even death.<sup>5</sup> Therefore, it is desirable to have fast, precise, and accurate analytical methods that can detect ethanol fuel adulteration by methanol on AEHC samples.

The use of vibrational spectroscopy (Fourier transform mid-infrared (FTMIR), Fourier transform near-infrared (FTNIR), FT-Raman) combined with multivariate analysis has proved to be a powerful tool in the evaluation of fossil fuels<sup>6–10</sup> and biofuels<sup>11–15</sup> quality control as well as in the analysis of ethanol and methanol in beverages.<sup>16–18</sup> Despite the fact that vibrational spectroscopy has already been used in the determination of

(4) Kaphalia, B. S.; Carr, J. B.; Ansari, G. A. S. *Fundam. Appl. Toxicol.* **1995**, 28, 264–273.

(5) Megarbane, B.; Borron, S. W.; Baud, F. J. *Intens. Care Med.* **2005**, 31, 189–195.

(6) Pereira, R. C. C.; Skrobot, V. L.; Castro, E. V. R.; Fortes, I. C. P.; Pasa, V. M. D. *Energy Fuels* **2006**, 20, 1097–1102.

(7) Johnson, K. J.; Morris, R. E.; Rose-Pehrsson, S. L. *Energy Fuels* **2006**, 20, 727–733.

(8) Santos, V. O.; Oliveira, F. C. C.; Lima, D. G.; Petry, A. C.; Garcia, E.; Suarez, P. A. Z.; Rubim, J. C. *Anal. Chim. Acta* **2005**, 547, 188–196.

(9) Oliveira, F. C. C.; de Souza, A.; Dias, J. A.; Dias, S. C. L.; Rubim, J. C. *Quim. Nova* **2004**, 27, 218–225.

(10) Iob, A.; Buenafe, R.; Abbas, N. M. *Fuel* **1998**, 77, 1861–1864.

(11) Oliveira, F. C. C.; Brandao, C. R. R.; Ramalho, H. F.; da Costa, L. A. F.; Suarez, P. A. Z.; Rubim, J. C. *Anal. Chim. Acta* **2007**, 587, 194–199.

(12) Felizardo, P.; Baptista, P.; Uva, M. S.; Menezes, J. C.; Correia, M. J. N. *J. Near Infrared Spectrosc.* **2007**, 15, 97–105.

(13) Felizardo, P.; Baptista, P.; Menezes, J. C.; Correia, M. J. N. *Anal. Chim. Acta* **2007**, 595, 107–113.

(14) Oliveira, J. S.; Montalvao, R.; Daher, L.; Suarez, P. A. Z.; Rubim, J. C. *Talanta* **2006**, 69, 1278–1284.

(15) Ghesti, G. F.; de Macedo, J. L.; Braga, V. S.; de Souza, A.; Parente, V. C. I.; Figueredo, E. S.; Resck, I. S.; Dias, J. A.; Dias, S. C. L. *J. Am. Oil Chem. Soc.* **2006**, 83, 597–601.

(16) Lachenmeier, D. W. *Food Chem.* **2007**, 101, 825–832.

\* Corresponding author. E-mail: hcarneiro@anp.gov.br.

† Agência Nacional do Petróleo (ANP).

‡ Universidade de Brasília.

(1) Eaves, J.; Eaves, S. *Energy Policy* **2007**, 35, 5958–5963.

(2) Cheremisinoff, N. P. *Industrial Solvents Handbook*, 2nd ed.; Marcel Dekker, Inc: New York, 2003.

(3) Ari, S.; Caca, I.; Kayabasi, H. *Ann. Ophthalmol.* **2007**, 39, 249–252.

**Table 1.** Composition of Standards (% w/w) Used for GC-FID Analysis

sample	water <sup>a</sup>	EtOH	MeOH	<i>t</i> -ButOH
1	0.00	89.70	0.00	10.30
2	7.50	60.24	21.84	10.42
3	6.57	37.35	44.55	11.53
4	6.44	18.50	64.52	10.54
5	0.00	0.00	91.37	8.63

<sup>a</sup> Water was added in order that these samples be similar to those used in the validation.

methanol in beverages, this application in the detection of methanol in AEHC or even in anhydrous ethanol has not been investigated yet.

Therefore, the aim of this work is to design calibration models based on partial least-squares (PLS) multivariate analysis combined with vibrational spectroscopy (FTMIR and FTNIR) to simultaneously quantify methanol, ethanol, and water in AEHC samples. The respective accuracies of the PLS models will be evaluated based on a gas chromatography flame ionization detection (GC-FID) reference method in order to establish which vibrational spectroscopic method presents the best accuracy.

### Experimental Details

**Chemicals.** Anhydrous ethanol (99.8% purity) and methanol (99.8% purity) were obtained from commercial sources (Vetec and CRQ) and used as received.

**Sample Preparation.** The ANP established that water content in AEHC samples cannot exceed 7.4% w/w.<sup>19</sup> In order to simulate AEHC samples adulterated with water and methanol, 80 synthetic samples were prepared by mixing anhydrous ethanol, methanol and water in different proportions. The water, ethanol, and methanol contents in the 80 samples varied at random intervals: 0–20% (water), 0–100% (ethanol), and 0–100% (methanol). These samples were prepared by weighing in an analytical balance (Mettler,  $\pm 0.0001$  g), and each sample has a final mass of 25.0 g. From the above 80 samples, 60 were used to design the PLS calibration models and 20 were separated for validation. It is worth mentioning that the reference values considered for this validation are those obtained by weighing in an analytical balance.

The set of 20 validation samples were also analyzed by GC-FID using calibration curves. Before GC analysis, 0.1 g of *t*-butanol (*t*-ButOH) as internal standard was added to an aliquot of 1.0 g of each sample. The GC calibration curves (for methanol and ethanol) were obtained using five multicomponent standards with compositions as displayed in Table 1.

**Instrumentation and Software.** The FT-NIR and FT-IR spectra were obtained on an Equinox 55 Fourier transform instrument from Bruker. The FTNIR spectra were recorded using an immersion transreflectance accessory coupled to a Ge detector (not cooled) by an optical fiber covering the 4000–14 000  $\text{cm}^{-1}$  spectral range. The optical path was 1 mm. The nominal spectral resolution was set to 8  $\text{cm}^{-1}$ , and each spectrum corresponds to the average of 16 scans. The FTMIR spectra were recorded using a horizontal ATR cell (ZnSe), 7 cm long (10 reflections), from Pike Technologies, covering the 650–4000  $\text{cm}^{-1}$  spectral range, using a DTGS detector. Each spectrum corresponds to the average of 32 scans with a 4  $\text{cm}^{-1}$  of a nominal spectral resolution. Three spectra were collected from each sample.

The PLS calibration models were obtained by the Quant2 (PLS1) method included in the OPUS software.

(17) Mendes, L. S.; Oliveira, F. C. C.; Suarez, P. A. Z.; Rubim, J. C. *Anal. Chim. Acta* **2003**, 493, 219–231.

(18) Perez-Ponce, A.; Rambla, F. J.; Garrigues, J. M.; Garrigues, S.; de la Guardia, M. *Analyst* **1998**, 123, 1253–1258.

(19) [http://nxt.anp.gov.br/NXT/gateway.dll/leg/resolucoes\\_anp/2005/dezembro/ranp%2036%20-%202005.xml?f=templates\\$fn=default.htm&sync=1&vid=anp:10.1048/enu](http://nxt.anp.gov.br/NXT/gateway.dll/leg/resolucoes_anp/2005/dezembro/ranp%2036%20-%202005.xml?f=templates$fn=default.htm&sync=1&vid=anp:10.1048/enu).

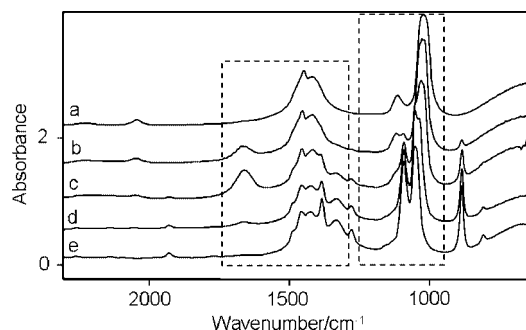


**Figure 1.** FTMIR spectra of five representative samples: (a) MeOH 100%; (b) MeOH 81.5%, EtOH 8.8%; (c) MeOH 46.9%, EtOH 34.8%; (d) MeOH 20.10%, EtOH 66.20%; and (e) EtOH 100%.

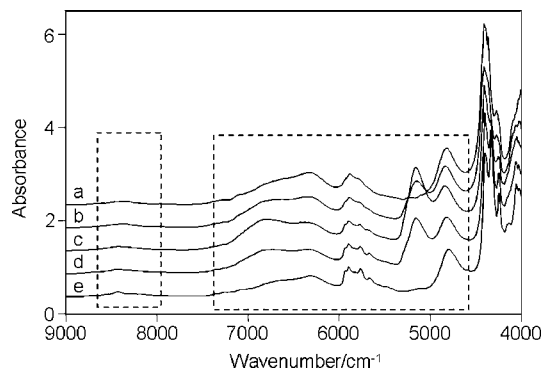


**Figure 2.** FTNIR spectra of five representative samples: (a) MeOH 100%; (b) MeOH 81.5%, EtOH 8.8%; (c) MeOH 46.9%, EtOH 34.8%; (d) MeOH 20.10%, EtOH 66.20%; and (e) EtOH 100%.

The chromatograms were obtained by GC on a Shimadzu GC-17A chromatograph with flame ionization detector, equipped with a polydimethylsiloxane column (CBPI PONA-M50-042) 50 m, 0.25 mm i.d., and film thickness of 0.2  $\mu\text{m}$ , working between 60 and 110  $^{\circ}\text{C}$ , with a heating rate of 10  $^{\circ}\text{C min}^{-1}$ , and standing at the final temperature for 5 min. The injector and detector temperatures were 250  $^{\circ}\text{C}$ .

### Results and Discussion

#### PLS Calibration Models Based on FTMIR and FTNIR.

FTMIR and FTNIR spectra of five representative samples used in the calibration models are displayed in Figures 1 and 2, respectively. In order to choose the spectral regions used to design the models, we have first calculated the spectral distribution of the relative standard deviation in the absorbance ( $\sigma_A/A$ ) for a set of 20 spectra of one representative sample. The spectral regions selected were those with the best signal-to-noise ratio, i.e., those with the smallest values of  $\sigma_A/A$ .<sup>9,17</sup> Then, we have also calculated the spectral distribution of the standard deviation in the absorbance ( $\sigma_A$ )<sup>8</sup> for the set of 80 samples. From the above selected regions, a fine adjustment was done by choosing the regions with the largest values of  $\sigma_A$ , the spectral regions that present the largest variability from sample to sample. The spectral regions selected as described above are: (i) FTMIR 840–1180  $\text{cm}^{-1}$  covering the C–O and C–C–O stretching modes; 1200–1750  $\text{cm}^{-1}$  covering the  $\text{CH}_2$ ,  $\text{CH}_3$ , C–OH, and HOH bending modes and (ii) FTNIR 4444–7460  $\text{cm}^{-1}$  covering the OH bending + OH stretching combination, the first overtones of CH and OH stretching modes, and 7935–8525  $\text{cm}^{-1}$  covering the second overtones of CH stretching. The selected regions used to design the PLS calibrations models are marked with rectangles in Figures 1 and 2. In order to verify if the selected spectral regions are relevant, PLS models including the whole spectral regions were also designed.

**Table 2. PLS Statistical Parameters for FTMIR and FTNIR Calibration and Validation and the *F*-Test Values for the Models Being Compared, Whole Spectra and Selected Regions<sup>a</sup>**

models		selected region				whole spectra				$F_{\text{value}}^e$	$y_D^d$ (% w/w)
		calibration		validation		calibration		validation			
		$R^2$	RMSEE	$R^2$	RMSEP <sub>2</sub>	$R^2$	RMSEE	$R^2$	RMSEP <sub>1</sub>		
FTMIR <sup>b</sup>	Water	99.99 (9)	0.17	99.44 (9)	0.31	99.90 (9)	0.18	99.30 (9)	0.35	1.25	0.37
	EtOH	99.98 (10)	0.33	99.95 (10)	0.42	99.99 (6)	0.31	99.86 (6)	0.77	3.07	0.71
	MeOH	99.98 (10)	0.37	99.93 (10)	0.52	99.87 (4)	0.98	99.71 (4)	1.09	4.33	0.77
FTNIR <sup>c</sup>	Water	99.99 (7)	0.05	99.98 (7)	0.06	99.97 (2)	0.09	99.98 (2)	0.07	1.34	0.10
	EtOH	99.99 (8)	0.25	100.0 (8)	0.13	99.99 (10)	0.31	99.98 (10)	0.28	4.70	0.53
	MeOH	99.99 (8)	0.24	99.99 (8)	0.15	99.99 (10)	0.31	99.98 (10)	0.31	3.97	0.50

<sup>a</sup> Values in parenthesis are the number of principal components; *R*<sup>2</sup> = coefficient of determination; RMSEE and RMSEP are the root mean square errors of estimation and prediction, respectively, preprocessing. <sup>b</sup> 1st derivative + MSC. <sup>c</sup> No preprocessing. <sup>d</sup> The *y*<sub>D</sub> values were calculated using eq 2 only for the PLS models considering the selected spectral regions. <sup>e</sup> See text for details.

The PLS calibration models based on the FTMIR and FTNIR spectroscopy were designed using 60 samples, and the other 20 samples were used in the test group. The statistical parameters of calibration and test set validation for these models are displayed in Table 2.

**Model Comparison.** The *F*-test<sup>20</sup> was used to compare the performances of the PLS calibration models considering the selected spectral regions and the whole spectra, for both FTMIR and FTNIR. The *F*-values were obtained by eq 1:

$$F = \frac{\text{RMSEP}_1^2}{\text{RMSEP}_2^2} \quad (1)$$

where RMSEP<sub>1</sub> and RMSEP<sub>2</sub> squared are the variances for the models being compared. The results are presented in Table 2.

The theoretical *F*-value for 19 degrees of freedom (df) (20 samples used in the validation) was not found in the literature. For a 95% of confidence level, the theoretical value for 15 and 20 df are 2.16 and 2.23, respectively.<sup>20</sup> It is reasonable to assume that the *F*-value for 19 df at a 95% confidence level will fall in the 2.16–2.23 interval. Therefore, for values within this interval, it will not be possible to draw any conclusion.

The results of Table 2 shows that, for both FTMIR and FTNIR, the differences between the RMSEP values obtained in the validation considering the selected spectral regions and the whole spectra are not statistically significant for water. However, the differences in RMSEP for methanol and ethanol are statistically significant, showing that the PLS models based on selected spectral regions should be used in the detection of methanol adulteration.

Ortiz et al.<sup>21</sup> have extended the application of the ISO 11843-2 norm<sup>22</sup> to evaluate the minimum detectable net concentration, *y*<sub>D</sub>, for multivariate calibration methods such as PLS. Accordingly, the *y*<sub>D</sub> values were evaluated by eq 2:

$$y_D = \delta_{\alpha,\beta,v} \frac{s}{b} \sqrt{\frac{1}{L} + \frac{1}{n} + \frac{\bar{y}^2}{\sum_{i=1}^L (y_i - \bar{y})^2}} \quad (2)$$

Where, *s* is the standard deviation of the residuals (*s* = RMSEE) of the calibration curve, in which the estimated concentration follows a linear dependence with the concentration of standards

**Table 3. *F*-Test Values for FTMIR vs FTNIR, FTMIR vs GC, and FTNIR vs GC**

compound	<i>F</i> -test values		
	FTMIR vs FTNIR	GC vs FTMIR	GC vs FTNIR
water	30.62		
ethanol	12.01	1.15	11.98
methanol	12.55	1.00	12.02

with a slope *b*, *L* is the number of standards, *n* is the number of replicate measurements performed on each sample,  $\bar{y}$  is the mean concentration of the standards, and  $\delta_{\alpha,\beta,v}$  is the noncentrality parameter from the noncentral *t*-distribution with probabilities  $\alpha$  and  $\beta$ , considering  $\nu = L - 2$  as the degrees of freedom of the calibration curve. In eq 2, we have used  $\delta = 3.32759$  for  $\alpha$  and  $\beta$  probabilities of 0.05 (95% of confidence level) as obtained from ref 23. The obtained *y*<sub>D</sub> values for the PLS models considering the selected spectral regions are displayed in Table 2. These values are all above the minimum concentration of standards. For instance, *y*<sub>D</sub> for MeOH as determined by the PLS/FTNIR model is  $0.50 \pm 0.15$  (% w/w) while the minimum concentration of MeOH in the standards was 0.0 (% w/w).

The 20 samples of the test group were also analyzed by GC to determine the methanol and ethanol contents. The GC results were obtained from calibration curves (see Figure 1S of the Supporting Information). The MeOH and EtOH contents of the 20 validation samples were determined using these calibration curves. The recovered MeOH or EtOH contents vs the real concentrations (obtained by weighing) provide linear correlations (see Figure 2S of the Supporting Information) with standard errors of prediction (SEP<sub>GC</sub>) for the methanol and ethanol contents of 0.52 and 0.45 (% w/w), respectively. The real (or expected) values, as weighed, and the recovered values of water, methanol, and ethanol contents (in % w/w), as obtained by the PLS-FTMIR and PLS-FTNIR calibration models and those obtained by GC are displayed in Table 1S of the Supporting Information. It is worth mentioning that the SEP<sub>GC</sub> values were used to obtain the *F*-values displayed in Table 3. In this sense, the *F*-value when comparing the FTNIR and FTMIR models was obtained by the ratio of the respective squared RMSEP values. The *F*-value for the PLS/FTNIR vs GC analysis was obtained by the ratio  $F = \text{SEP}_{\text{GC}}^2 / \text{RMSEP}_{\text{NIR}}^2$ , where SEP<sub>GC</sub><sup>2</sup> and RMSEP<sub>NIR</sub><sup>2</sup> are the variances of the GC and NIR validation results.

The results of Table 3 show that differences between the RMSEP values (PLS models) and the SEP<sub>GC</sub> are statistically significant for PLS/FTNIR models but not for PLS/FTMIR models. This means that the use of the PLS/FTNIR model should be recommended for methanol detection in AEHC, since this model presents smaller prediction errors. Comparisons for the content of water were not possible because GC-FID cannot determine it.

(20) Freund, J. E.; Simon, G. A. *Modern Elementary Statistics*; Prentice-Hall, Inc.: Upper Saddle River, NJ, 1997.

(21) Ortiz, M. C.; Sarabia, L. A.; Herrero, A.; Sánchez, M. S.; Sanz, M. B.; Rueda, M. E.; Giménez, D.; Meléndez, M. E. *Chemom. Intell. Lab. Syst.* **2003**, *69*, 21.

(22) ISO 11843-2; *Capability of detection*; International Standards Organization: Geneva, Switzerland; 2000.

(23) Clayton, C. A.; Hines, J. W.; Elkins, P. D. *Anal. Chem.* **1987**, *59*, 2506.

The results of the first column of Table 3 make also possible the comparison between the two PLS models. The larger values of  $F$  indicate that the FTNIR models present the smallest values of RMSEP and therefore better accuracy for the determination of water, ethanol, and methanol in AEHC.

### Conclusion

The results obtained in this work lead us to conclude:

(i) FTMIR as well as FTNIR spectroscopy can be used to determine the adulteration of AEHC with methanol. The accuracies of the PLS models obtained depend on the spectroscopic technique used. By an appropriate choice of spectral regions, it has been shown that PLS/FTNIR calibration models are able to determine the adulteration of AEHC with methanol with accuracy better than 0.16% w/w, while for PLS/FTMIR the accuracy was better than 0.55% w/w.

(ii) The minimum detected net concentrations for water, EtOH, and MeOH by the PLS models were below 1% w/w for both spectroscopic techniques.

(iii) The PLS/FTNIR models presented better accuracies than the GC-FID reference method. Therefore, due to their faster response, good precision, and remote sensing capability, this method should be used in the monitoring process of AEHC adulteration by methanol.

**Acknowledgment.** The authors thank ANP for encouragement. The authors thank Finep/CTPETRO, Finep/CTEnerg, Finatec, and CNPq for financial support. F.C.C.O., P.A.Z.S., and J.C.R. thank CNPq for research fellowships.

**Supporting Information Available:** Table 1S with the contents (in percent w/w) of water, ethanol, and methanol as real and predicted by FTMIR, FTNIR, and GC-FID; Table 2S with the slopes of the PLS calibration curves and the standard deviation of triplicate measurements; Figure 1S with the GC-FID calibration curves for MeOH and EtOH; and Figure 2S with the plots of MeOH and EtOH concentrations recovered by GC analysis vs the real concentrations. This material is available free of charge via the Internet at <http://pubs.acs.org>.

EF8000218